FORMATION CONTROL OF MULTI-ROBOTS VIA SLIDING-MODE TECHNIQUE

Razvan Solea, Daniela Cernega, Adrian Filipescu and Adriana Serbencu
Control Systems and Industrial Informatics Department, Computer Science Faculty
"Dunarea de Jos" University of Galati, Domneasca 111, 800201, Galati, Romania

Keywords: Formation control, Sliding-mode control, Skid-steering mobile robot.

Abstract: This paper addresses the control of a team of nonholonomic mobile robots. Indeed, the most work, in this domain, have studied extensively classical control for keeping a formation of mobile robots. In this work, the leader mobile robot is controlled to follow an arbitrary reference path, and the follower mobile robot use the sliding-mode controller to keep constant relative distance and constant angle to the leader robot. The efficiency and simplicity of this control laws has been proved by simulation on different situations.

1 INTRODUCTION

The multi robots systems is an important robotics research field. Such systems are of interest for many reasons; tasks could be too complex for a simple robot to accomplish; using several simple robots can be easier, cheaper and more flexible than a single powerful robot (Mazo et al., 2004), (Zavlanos and Pappas, 2008), (Murray, 2007), (Liu et al., 2007), (Klančar et al., 2009).

Formation control has been one of the important research topics in multiple robot systems as it is applicable to many areas such as geographical exploration, rescue operations, surveillance, mine sweeping, and transportation. Different approaches have been developed recently, for example, behavior-based control, LQ control, visual servoing control, Lyapunov-based control, input and output feedback linearization control, graph theory, and nonlinear control.

In leader-follower formation control, the most widely used control technique is feedback linearization based on the kinematics model of the system. In this study, we focus on the problem of leader-follower robot formation control using a sliding-mode controller.

The referenced robot is called a leader, and the robot following it called a follower. Thus, there are many pairs of leaders and followers and complex formations can be achieved by controlling relative positions of these pairs of robots respectively. This approach is characterized by simplicity, reliability and no need for global knowledge and computation.

Figure 1: A skid-steered four wheel mobile robot.

In this paper, it will be developped a method based on the leader-following approach to investigate formation control problem in a group of nonholonomic mobile robots. For this purpose, we design a new controller based on sliding-mode control to drive a fleet of mobile robots in a leader-follower configuration.

Sliding Mode Control (SMC) method has been widely noticed because of its superior robust control performance for systems with highly uncertainty (Chwa, 2004), (Yang and Kim, 1999), (Floquet et al., 2003), (Solea and Nunes, 2007), (Solea and Cernega, 2009).

The rest of this paper is organized as follows. First formulation of the nonholonomic mobile robot system is revealed. Then, the leader-following formation model method used by the robots is exposed. After that, the architecture of the siling-mode controller is described. This paper concludes with some simulation and results.

Solea R., Cernega D., Filipescu A. and Serbencu A. (2010).
FORMATION CONTROL OF MULTI-ROBOTS VIA SLIDING-MODE TECHNIQUE.
In *Proceedings of the 7th International Conference on Informatics in Control, Automation and Robotics*, pages 161-166
DOI: 10.5220/0002899501610166

2 FORMATION CONTROL

2.1 Formulation of the Nonholonomic Mobile Robot System

As indicated in Figure 1, the mobile robots are skid-steering mobile platforms. To develop the kinematic model for a skid-steering mobile robot (SSMR) that is assumed to move in a plane (for simplicity) with an inertial coordinate system, denoted by $(X_g,\ Y_g)$, and a local coordinate system, denoted by $(X_r,\ Y_r)$, where the origin of $(X_r,\ Y_r)$ is fixed to the center of mass (CG) of the SSMR as illustrated in Figure 2. The position and orientation of the CG, denoted by $q(t) \in R^3$, is defined as $q = [x_r\ y_r\ \theta_r]^T$ (i.e., the CG position, x_r and y_r, and the orientation θ_r of the local coordinate frame with respect to the inertial frame).

$$\begin{bmatrix} \dot{x}_r \\ \dot{y}_r \\ \dot{\theta}_r \end{bmatrix} = \begin{bmatrix} cos(\theta_r) & -sin(\theta_r) & 0 \\ sin(\theta_r) & cos(\theta_r) & 0 \\ 0 & 0 & 1 \end{bmatrix} \cdot \begin{bmatrix} v_{xr} \\ v_{yr} \\ \omega_r \end{bmatrix} \tag{1}$$

It is obvious that Eqn. (1) does not impose any restrictions on the skid-steering mobile robot plane movement, since it describes free-body kinematics only. Therefore it is necessary to analyze the relationship between wheel velocities and local velocities.

Suppose that the $i-th$ wheel rotates with an angular velocity $\omega_{ir}(t)$, where $i = 1,2,...,4$, which can be seen as a control input. For simplicity, the thickness of the wheel is neglected and is assumed to be in contact with the plane at point P_{ir} as illustrated in Figure 3. In contrast to most wheeled vehicles, the lateral velocity of the SMRR, v_{iyr}, is generally nonzero. This property comes from the mechanical structure of the SSMR that makes lateral skidding necessary if the vehicle changes its orientation. Therefore the wheels are tangent to the path only if $\omega_r = 0$, i.e., when the robot moves along a straight line.

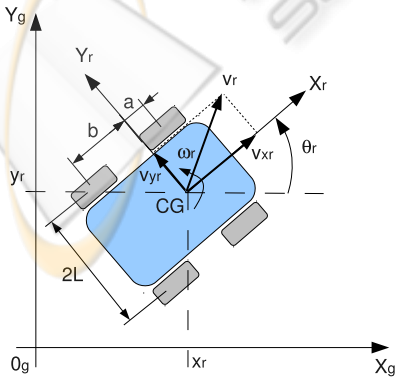

Figure 2: Free body diagram.

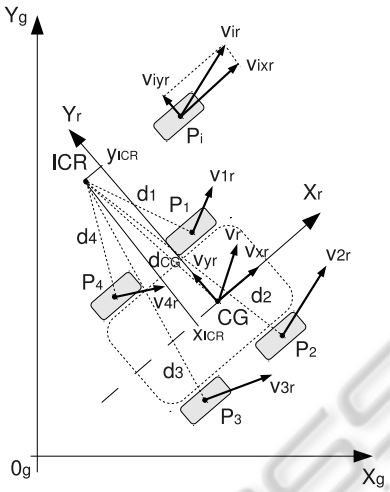

Figure 3: Wheel velocities.

In this description we consider only a simplified case of the SSMR movement for which the longitudinal slip between the wheels and the surface can be neglected. For traditional mobile robots, the wheel rotation is translated into a linear motion along the tangent of a curve without longitudinal slippage as described by the following expressions:

$$v_{ixr} = R_i \cdot \omega_i \tag{2}$$

where v_{ixr} is the longitudinal component of the total velocity vector v_{ir} of the $i-th$ wheel expressed in the local frame and R_i denotes the so-called effective rolling radius of that wheel.

The vectors $d_i(t) = [d_{ix}(t), d_{iy}(t)]^T$ and $d_{CG}(t) = [d_{CGx}(t), d_{CGy}(t)]^T \in R^2$ are expressed in (X_r, Y_r) and are defined from the instantaneous center of rotation (ICR) of the vehicle to $P_i\ \forall i = 1,2,...,4$ and $d_{CG}(t)$ from the ICR to the vehicle to CG, respectively, as illustrated in Figure 3. Based on the geometry of Figure 3, the following expressions can be developed:

$$\frac{v_{ixr}}{d_{iy}} = \frac{v_{xr}}{y_{ICR}} = \frac{v_{iyr}}{d_{ix}} = -\frac{v_{yr}}{x_{ICR}} = \omega_r \tag{3}$$

where it is used the fact that the coordinates of the ICR expressed in (X_r, Y_r), denoted by $x_{ICR}(t)$ and $y_{ICR}(t) \in R$, are defined as $[x_{ICR}, y_{ICR}]^T = [-d_{CGx}, d_{CGy}]^T$.

From Figure 3 it is clear that the coordinates of vectors d_{ir} satisfy the following relationships:

$$\begin{aligned} d_{1y} &= d_{4y} = d_{CGy} - L \\ d_{2y} &= d_{3y} = d_{CGy} + L \\ d_{1x} &= d_{2x} = d_{CGx} + a \\ d_{3x} &= d_{4x} = d_{CGx} - b \end{aligned} \tag{4}$$

After combining Eqns. (3) and (4), the following relationships between wheel velocities can be obtained:

$$\begin{aligned} v_L &= v_{1xr} = v_{4xr} \quad v_R = v_{2xr} = v_{3xr} \\ v_F &= v_{1yr} = v_{2yr} \quad v_B = v_{3yr} = v_{4yr} \end{aligned} \tag{5}$$

where v_L and v_R denote the longitudinal coordinates of the left and right wheel velocities, v_F and v_B are the lateral coordinates of the velocities of the front and rear wheels, respectively.

Using (3) - (5) it is possible to obtain the following transformation describing the relationship between the wheel velocities and the velocity of the robot:

$$\begin{bmatrix} v_L \\ v_R \\ v_F \\ v_B \end{bmatrix} = \begin{bmatrix} 1 & -L \\ 1 & L \\ 0 & -x_{ICR}+a \\ 0 & -x_{ICR}-b \end{bmatrix} \cdot \begin{bmatrix} v_{xr} \\ \omega_r \end{bmatrix} \quad (6)$$

Notice that ω_L and ω_R which denote angular velocities of left and right wheels, respectively, can be regarded as control inputs at kinematic level and can be used to control longitudinal and angular velocity according to the following relationships:

$$v_{xr} = R \cdot \frac{\omega_R + \omega_L}{2}, \ \omega_r = R \cdot \frac{\omega_R - \omega_L}{2 \cdot L} \quad (7)$$

while R is so called effective radius of wheels and $2 \cdot L$ is a spacing wheel track depicted in Figure 2.

It is interesting to see that the analysed kinematic model of the SSMR is quite similar to the kinematics of the two-wheel mobile robot.

From the last equations it is clear that, theoretically, the pair of velocities ω_L and ω_R can be treated as a control kinematic input signal as well as velocities v_{xr} and ω_r. However, the accuracy of the relations (7) mostly depends on the longitudinal slip and can be valid only if this phenomenon is not dominant. In addition, the parameters R and L may be identified experimentally to ensure a high validity of the determination of the angular robot velocity with respect to the angular velocities of the wheels.

To complete the kinematic model of the SSMR, the following velocity constraint can be considered:

$$v_{yr} + x_{ICR} \cdot \omega_r = 0 \quad (8)$$

The last equation is not integrable. In consequence, it describes a nonholonomic constraint which can be rewritten like:

$$\begin{bmatrix} -sin(\theta_r) & cos(\theta_r) & x_{ICR} \end{bmatrix} \cdot \begin{bmatrix} \dot{x}_r \\ \dot{y}_r \\ \dot{\theta}_r \end{bmatrix} = 0 \quad (9)$$

2.2 Leader-follower Formation Models

Figure 4 is a leader-follower control model where the formation pattern is specified by the separate distance d and the relative bearing ψ for two robots $r1$ and $r2$. The desired formation pattern can be defined as the desired separate distance d^d and the relative bearing

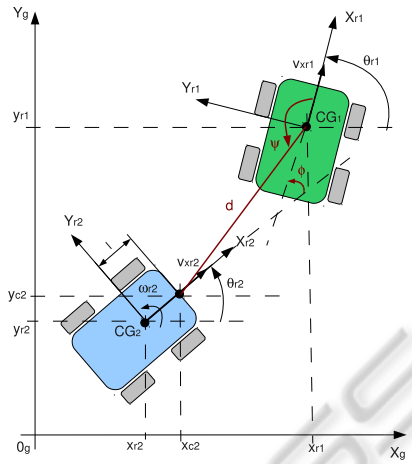

Figure 4: Leader-follower approach for SSMR.

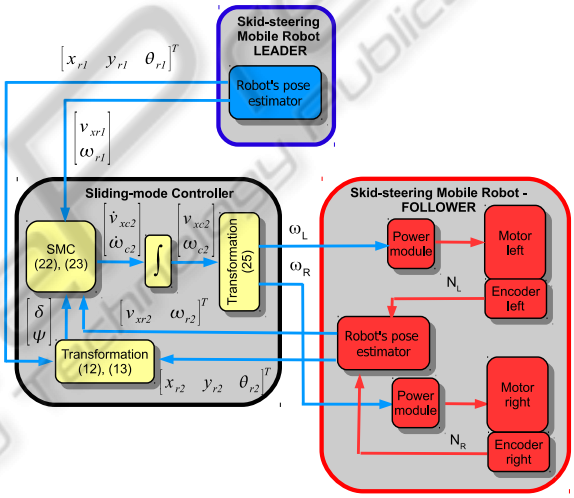

Figure 5: Block diagram.

ψ^d. The follower $r2$ regulates the formation state errors of the separate distance and the relative bearing through its speed control signals $u_{r2} = [v_{xr2}, \omega_{r2}]^T$:

$$\begin{bmatrix} \tilde{d} \\ \tilde{\psi} \end{bmatrix} = \begin{bmatrix} d^d \\ \psi^d \end{bmatrix} - \begin{bmatrix} d \\ \psi \end{bmatrix} \quad (10)$$

The relative distance between the leader and the follower robot is denoted as d, the separation bearing angle is ψ, and they are given by:

$$d = \sqrt{(x_{r1} - x_{c2})^2 + (y_{r1} - y_{c2})^2} \quad (11)$$

$$\psi = \pi - [\theta_{r1} - arctan2(y_{r1} - y_{c2}, x_{r1} - x_{c2})] \quad (12)$$

where:

$$x_{c2} = x_{r2} + l \cdot cos(\theta_{r2}), \ \ y_{c2} = y_{r2} + l \cdot sin(\theta_{r2})$$

The formation control can be investigated by modeling the formation state error as follows (Das et al.,

2002):

$$\begin{bmatrix} \dot{\tilde{d}} \\ \dot{\tilde{\psi}} \end{bmatrix} = G \cdot u_{r2} + F \cdot u_{r1},\ \dot{\phi} = \omega_{r1} - \omega_{r2} \qquad (13)$$

and

$$G = \begin{bmatrix} -cos(\phi+\psi) & -l \cdot sin(\phi+\psi) \\ \frac{sin(\phi+\psi)}{d} & -\frac{l \cdot cos(\phi+\psi)}{d} \end{bmatrix},$$

$$F = \begin{bmatrix} cos(\psi) & 0 \\ -\frac{sin(\psi)}{d} & 1 \end{bmatrix}$$

where $\phi = \theta_{r1} - \theta_{r2}$ and l is the distance between the robot position (x_{r2}, y_{r2}) and the robot hand position (x_{c2}, y_{c2}) as shown in Figure 4.

2.3 Sliding-mode Controller Design

In a leader-follower configuration, with the leader's position given and once the follower's relative distance and angle with respect to the leader are known, the follower's position can be determined. To use the leader-following approach, it is assumed that the angular and linear velocities of the leader are known. In order to achieve and maintain the desired formation between the leader and follower, it is only need to control the follower's angular and linear velocities to achieve the relative distance and angle between them as specified. Therefore, the leader-following based mobile robot formation control can be considered as an extension of the tracking control problem of the nonholonomic mobile robot.

A practical form of reaching the control law (proposed by Gao and Hung (Gao and Hung, 1993)) is defined as

$$\dot{s}_i = -p_i \cdot |s_i|^{\alpha} \cdot sgn(s_i),\ 0 < \alpha < 1,\ i = 1,2 \qquad (14)$$

This reaching law increases the reaching speed when the state is far away from the switching manifold, but reduces the rate when the state is near the manifold. The result is a fast reaching and low chattering reaching mode.

A new design of sliding surface is proposed, such that the separation bearing angle, ψ and the orientation error ϕ, are internally coupled with each other in a sliding surface leading to convergence of both variables. For that purpose the following sliding surfaces is proposed:

$$s_1 = \dot{\tilde{d}} + \gamma_d \cdot \tilde{d} \qquad (15)$$

$$s_2 = \dot{\tilde{\psi}} + \gamma_\psi \cdot \tilde{\psi} + \gamma_0 \cdot sgn(\tilde{\psi}) \cdot |\phi| \qquad (16)$$

here γ_0, γ_d, γ_ψ are positive constant parameters and $\tilde{d}$, $\tilde{\psi}$, ϕ are defined by (10), (13).

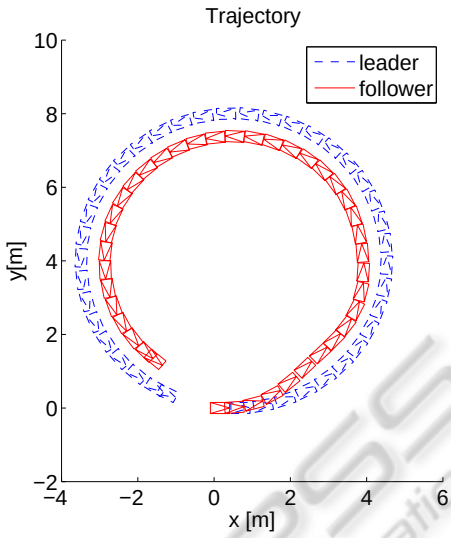

Figure 6: Simulation I - Trajectory of the leader and the follower.

If s_1 converges to zero, trivially $\tilde{d}$ converges to zero. If s_2 converges to zero, in steady-state it becomes $\dot{\tilde{\psi}} = -\gamma_\psi \cdot \tilde{\psi} - \gamma_0 \cdot sgn(\tilde{\psi}) \cdot |\phi|$. Since $|\phi|$ is always bounded, the following relationship between $\tilde{\psi}$ and $\dot{\tilde{\psi}}$ holds: $\tilde{\psi} < 0 \Rightarrow \dot{\tilde{\psi}} > 0$ and $\tilde{\psi} > 0 \Rightarrow \dot{\tilde{\psi}} < 0$.

From the time derivative of (15) and (16) and using the reaching law defined in (14) yields:

$$\dot{s}_1 = \ddot{\tilde{d}} + \gamma_d \cdot \dot{\tilde{d}} = -p_1 \cdot |s_1|^{\alpha} \cdot sgn(s_1) \qquad (17)$$

$$\dot{s}_2 = \ddot{\tilde{\psi}} + \gamma_\psi \cdot \dot{\tilde{\psi}} + \gamma_0 \cdot sgn(\tilde{\psi}) \cdot sgn(\tilde{\phi}) \cdot \dot{\phi} = \\ = -p_2 \cdot |s_2|^{\alpha} \cdot sgn(s_2) \qquad (18)$$

After some mathematical manipulation, one can achieve:

$$\dot{v}_{xc2} = \frac{p_1 \cdot |s_1|^{\alpha} \cdot sgn(s_1) + \gamma_d \cdot \dot{\tilde{d}} - D_1}{cos(\phi+\psi)} \qquad (19)$$

$$\dot{\omega}_{c2} = \frac{(p_2 \cdot |s_2|^{\alpha} \cdot sgn(s_2) + \gamma_{psi} \cdot \dot{\tilde{\psi}}) \cdot d - D_2}{l \cdot cos(\phi+\psi)} \qquad (20)$$

where

$D_1 = l \cdot \dot{\omega}_{r2} \cdot sin(\phi+\psi) - d \cdot (\dot{\phi}+\dot{\psi}) \cdot (\dot{\psi}+\omega_{r1}) - \\ -\dot{v}_{xr1} \cdot cos(\psi) - v_{xr1} \cdot \dot{\phi} \cdot sin(\psi)$

$D_2 = \gamma_0 \cdot sgn(\tilde{\psi} \cdot \phi) \cdot \dot{\phi} \cdot d - \dot{v}_{xr2} \cdot sin(\phi+\psi) + \\ +\dot{v}_{rx1} \cdot sin(\psi) - v_{xr1} \cdot \dot{\phi} \cdot cos(\psi) - (\dot{\phi}+\dot{\psi}) \cdot \dot{d} - \\ -d \cdot \dot{\omega}_{r1} - \dot{d} \cdot (\dot{\psi}+\omega_{r1})$

The *signum* functions in the sliding surface were replaced by *saturation* functions, to reduce the chattering phenomenon (Slotine and Li, 1991).

3 SIMULATION RESULTS

In this section, simulation results for the proposed SMC are presented. The simulation are performed

in Matlab/Simulink environment to verify behavior of the controlled system. The parameters of the SSMR model were chosen to correspond as closely as possible to the real experimental robot presented in section 1 in the following manner: $a = 0.10[m]$, $b = 0.20[m]$, $L = 0.12[m]$, $R = 0.04[m]$. Wheel velocity commands,

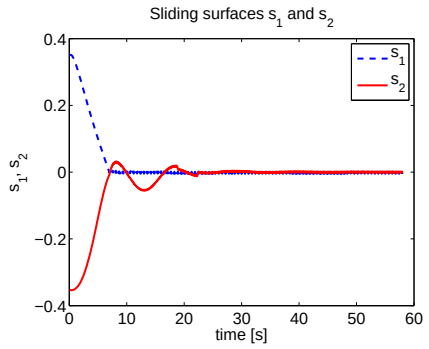

(a)

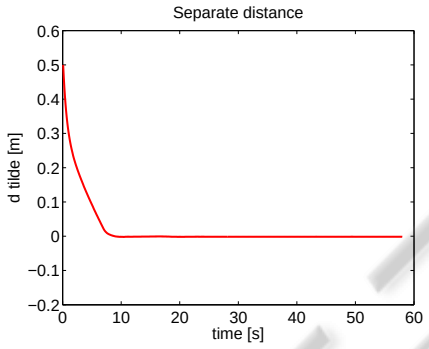

(b)

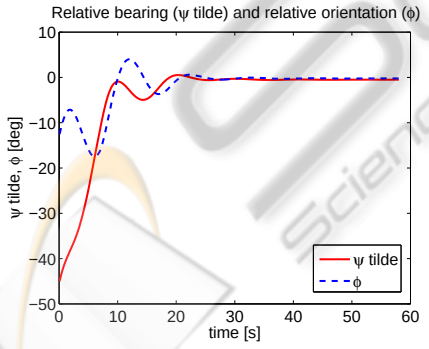

(c)

Figure 7: Simulation I - Sliding surfaces s_1 and s_2, separate distance ($\tilde{d}$), relative bearing ($\tilde{\psi}$) and relative orientation (ϕ).

$$\omega_R = \frac{v_{xc2} + L \cdot \omega_{c2}}{R}; \quad \omega_L = \frac{v_{xc2} - L \cdot \omega_{c2}}{R}; \qquad (21)$$

are sent to the power modules of the follower mobile robot, and encoder measures NR and NL are received in the robots pose estimator for odometric computations.

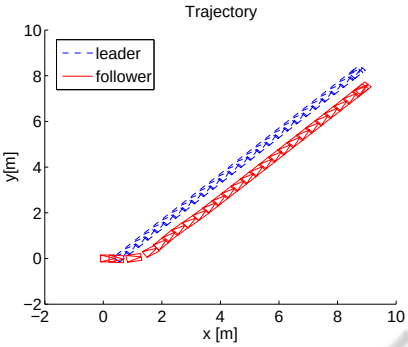

Figure 8: Simulation II - Trajectory of the leader and the follower.

Figure 5 shows a block diagram of the proposed sliding-mode controller.

In order to compute the actuating control input, equation (6) needs to be integrated and some initial values $v_{xc2}(0)$, $\omega_{c2}(0)$ to be fixed.

Two simulation experiments were carried out to evaluate the performance of the sliding mode controller presented in Section 2.3. The first simulation refers to the case of circular trajectory ($v_{xr1} = 0.4[m/s]$ and $\omega_{r1} = 0.1[rad/s]$). The initial conditions of the leader and the follower are, $x_{r1}(0) = 0.5$, $y_{r1}(0) = 0$, $\theta_{r1}(0) = 0$, $x_{r2}(0) = 0$, $y_{r2}(0) = 0$, $\theta_{r1}(0) = 0$, $d^d = 1.0[m]$, $\psi^d = 135[deg]$.

In the second simulation the leader robot execute a linear trajectory but with a non-zero initial orietation ($\theta_{r1} = 45[deg]$). The initial conditions of the leader and the follower in this second case are, $x_{r1}(0) = 0.5$, $y_{r1}(0) = 0$, $\theta_{r1}(0) = pi/4$, $x_{r2}(0) = 0$, $y_{r2}(0) = 0$, $\theta_{r1}(0) = 0$, $d^d = 1.0[m]$, $\psi^d = -120[deg]$.

Figure 6 shows the trajectory of the leader and the follower for the first simulation case. In order to have a temporal reference in the figure the robots are drawn each second: the blue car represent the leader and the red car represent the follower.

In Figure 7.a the sliding surfaces s_1 and s_2 asymptotically converge to zero. Finally, Figures 7.b and c show the time histories of $\tilde{d}$, $\tilde{\psi}$ and ϕ.

The results of the second case called Simulation II are given in Figures 8 - 9. Figure 8 shows the trajectory of the leader and the follower, Figures 9 the sliding surfaces and the time histories of $\tilde{d}$, $\tilde{\psi}$ and ϕ.

The good performance for controlling the formation with the developed control law can be observed from Figures 6 - 9. The outputs of the formation system ($\tilde{d}$, $\tilde{\psi}$ and ϕ) asymptotically converge to zero, as shown in Figures 7 and 9.

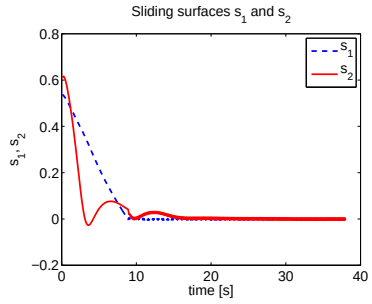

(a)

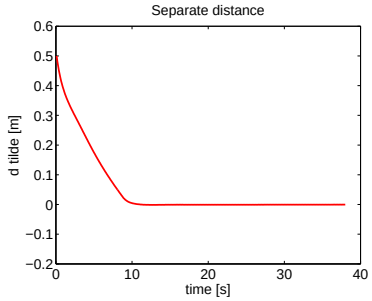

(b)

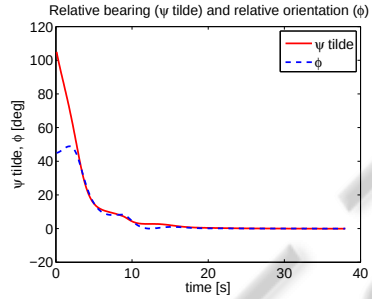

(c)

Figure 9: Simulation II - Sliding surfaces s_1 and s_2, separate distance ($\tilde{d}$), relative bearing ($\tilde{\psi}$) and relative orientation (ϕ).

4 CONCLUSIONS

In this paper is proposed a sliding mode formation tracking control scheme of nonholonomic mobile robots. The leader and follower are a skid-steering mobile robots. The desired formation, defined by two parameters (a distance and an orientation function) is allowed to vary in time. The effectiveness of the proposed designs has been validated via simulation experiments.

Future research lines include the experimental validation of our control scheme and the extension of our results to skid-steering mobile robots. For the sake of simplicity in the present paper a single-leader, single-follower formation has been considered. Future investigations will cover the more general case of multi-leader, multi-follower formations.

ACKNOWLEDGEMENTS

This work was supported by CNCSIS-UEFISCSU, projects PNII-IDEI 506/2008 and PNII-IDEI 641/2007.

REFERENCES

Chwa, D. (2004). Sliding-mode tracking control of nonholonomic wheeled mobile robots in polar coordinates. *IEEE Transactions on Control*, 12(4):637–644.

Das, A., Fierro, R., Kumar, V., Ostrowski, J., Spletzer, J., and Taylor, C. (2002). A vision-based formation control framework. *IEEE Transactions on Robotics and Automation*, 18(5):813–825.

Floquet, T., Barbot, J. P., and Perruquetti, W. (2003). Higher-order sliding mode stabilization for a class of nonholonomic perturbed systems. *Automatica*, 39(6):1077–1083.

Gao, W. and Hung, J. C. (1993). Variable structure control of nonlinear systems: A new approach. *IEEE Transactions on Industrial Electronics*, 40(1):45–55.

Klančar, G., Matko, D., and Blažič, S. (2009). Wheeled mobile robots control in a linear platoon. *Journal of Intelligent and Robotic Systems*, 54(5):709–731.

Liu, S.-C., Tan, D.-L., and Liu, G.-J. (2007). Robust leader-follower formation control of mobile robots based on a second order kinematics model. *Acta Automatica Sinica*, 33(9):947–955.

Mazo, M., Speranzon, A., Johansson, K., and Hu, X. (2004). Multi-robot tracking of a moving object using directional sensors. In *IEEE International Conference on Robotics and Automation, ICRA '04*, volume 2, pages 1103–1108.

Murray, R. M. (2007). Recent research in cooperative control of multi-vehicle systems. *Journal of Dynamic Systems, Measurement, and Control*, 129(5):571–583.

Slotine, J. J. E. and Li, W. (1991). *Applied Nonlinear Control*. Prentice-Hall.

Solea, R. and Cernega, D. (2009). Sliding mode control for trajectory tracking problem - performance evaluation. In *Lecture Notes in Computer Science, Springer*, volume 5769, pages 865–874.

Solea, R. and Nunes, U. (2007). Trajectory planning and sliding-mode control based trajectory-tracking for cybercars. *Aided Engineering, IOS Press*, 14(1):33–47.

Yang, J.-M. and Kim, J.-H. (1999). Sliding mode control for trajectory tracking of nonholonomic wheeled mobile robots. *IEEE Transactions on Robotics and Automation*, 15(3):578–587.

Zavlanos, M. M. and Pappas, G. J. (2008). Dynamic assignment in distributed motion planning with local coordination. *IEEE Transactions on Robotics*, 24(1):232–242.